

Modulation stability of wave-packets in a three-layer fluid

Kharchenko D. S., Naradovyi V. V.

*Volodymyr Vynnychenko Central Ukrainian State University,
1 Shevchenko Str., 25000, Kropyvnytskyi, Ukraine*

(Received 10 September 2021; Revised 5 December 2023; Accepted 5 December 2022)

This article investigates the modulation stability condition for the problem of wave packet propagation in a three-layer hydrodynamic system “layer with a hard bottom – layer – layer with a lid”. The graphs of the dependence of the modulation stability limits on the thickness of the lower and upper layer and on the density of the middle and upper layers for capillary and gravity waves are illustrated and analyzed. The evolution equations of the envelope of wave packets in the form of the second-order nonlinear Schrödinger equation for the lower and upper surfaces of the contact are obtained. The conditions of modulation stability are derived.

Keywords: *wave-packets; modulation stability; gravity waves.*

2010 MSC: 76A02, 76E30, 76B15

DOI: 10.23939/mmc2023.04.1292

1. Analysis of literature data

The study of the properties of waves and their stability in stratified liquids and the ocean is the subject of many modern studies.

A strongly nonlinear long wave model for large amplitude internal waves in a three-layer flow between two rigid boundaries is considered in [1]. Solitary-wave solutions of the model are shown to be governed by a Hamiltonian system with two degrees of freedom. Emphasis is placed on the solitary waves of the second baroclinic mode (mode-2) and their strongly nonlinear characteristics that fail to be captured by weakly nonlinear models.

In certain asymptotic limits relevant to oceanic applications and previous laboratory experiments, it is shown that large amplitude mode-2 waves with single-hump profiles can be described by the solitary-wave solutions of the MCC model. In case when the density stratification is weak and the density transition layer is thin, the richness of the dynamical system with two degrees of freedom becomes apparent and new classes of mode-2 solitary-wave solutions of large amplitudes, characterized by multi-humped wave profiles. In contrast with the classical solitary-wave solutions described by the MCC equation, such multi-humped solutions cannot exist for a continuum set of wave speeds for a given layer configuration. The analytical predictions based on asymptotic theory are then corroborated by a numerical study of the original Hamiltonian system.

In [2] interfacial internal waves in a stratified fluid excited by periodic free-surface perturbations in a closed tank are studied experimentally. Barotropic-baroclinic energy conversion is induced by the presence of a bottom obstacle. The connection between horizontal surface velocities and internal wave amplitudes is studied, the developing flow patterns are described qualitatively, and the wave speeds of internal waves are systematically analyzed and compared to linear two- and three-layer theories.

In the article [3] the theory of long nonlinear oscillating wave packets (breathers) in a stratified fluid with a small density difference in a gravitational field is developed. The theory is based on the Gardner equation and its modifications, which are completely integrable by modern methods of the nonlinear wave theory. Examples of the breather generation are given and the conditions for their stability are presented.

Article [4] discusses a new paradigm introduced by David J. Benney (an applied mathematician and fluid dynamicist whose highly original work has shaped the authors of the article understanding

of nonlinear wave and instability processes in fluid flows) in the study of nonlinear phenomena, which transcends fluid mechanics, and it highlights the common threads of his research contributions, namely, resonant nonlinear wave interactions; the derivation of nonlinear evolution equations, including the celebrated nonlinear Schrödinger equation for modulated wave trains; and the significance of three-dimensional disturbances in shear flow instability and transition.

Under consideration in paper [5] is the AB system describing marginally unstable baroclinic wave packets in geophysical fluids. By means of the n -fold modified Darboux transformation, the semirational solutions in terms of the determinants of the AB system are derived. The link between the baseband modulational instability and the existence condition of these rogue waves is revealed.

The work [6] is devoted to the study of stability and instability of periodic traveling waves for Korteweg-de Vries-type equations with fractional dispersion and related, nonlinear dispersive equations. It is shown that a local constrained minimizer for a suitable variational problem is nonlinearly stable to period preserving perturbations, provided that the associated linearized operator enjoys a Jordan block structure. The cases when the linearized equation admits solutions exponentially growing in time are discussed.

In the article [7] the modulational instability of two-dimensional nonlinear traveling-wave solutions of the Whitham equation in the presence of constant vorticity is considered. It is shown that vorticity has a significant effect on the growth rate of the perturbations and on the range of unstable wavenumbers. Waves with kh greater than a critical value, where k is the wave number of the solution and h is the fluid depth, are modulationally unstable. This critical value decreases as the vorticity increases. Additionally, it is found that waves with large enough amplitude are always unstable, regardless of wavelength, fluid depth, and strength of vorticity. These results are in qualitative agreement with those obtained by considering fully nonlinear solutions of the water-wave equations.

In the article [8] the scenario of resonant interactions as a result of which there can arise rogue waves modeled as special breathers (pulsating modes) for internal waves in the fluid stratified on density is considered. The properties of these rogue waves, such as the polarity, amplitude and stability, are studied, and it is shown that they critically depend on the specific density stratification and the choice of the participating modes. Three examples, namely, a two-layered fluid, a stratified fluid with constant buoyancy frequency, and a case of variable buoyancy frequency are examined.

It is shown that both elevation and depression rogue waves are possible, and the maximum displacements need not be confined to a fixed ratio of the background plane wave. Furthermore, there is no constraint on the signs of nonlinearity and dispersion, nor any depth requirement on the fluid. All these features contrast sharply with those of a wave packet evolving on water of finite depth governed by the nonlinear Schrödinger equation. For the case of constant buoyancy frequency, critical wave numbers give rise to nonlinear evolution dynamics for “long wave – short wave resonance”, and also separate the focusing and defocusing regimes for narrow-band wave packets of the nonlinear Schrödinger equation. Numerical simulations are performed by using baseband modes as initial conditions to assess the robustness of these rogue waves in relation to the modulation instability of a background plane wave.

The study [9] is concerned with the large time behavior of the two-dimensional compressible Navier–Stokes–Korteweg equations, using to model compressible fluids with internal capillarity. Based on the fact that the rarefaction wave, one of the basic wave patterns to the hyperbolic conservation laws is nonlinearly stable to the one-dimensional compressible Navier–Stokes–Korteweg equations, the planar rarefaction wave to the two-dimensional compressible Navier–Stokes–Korteweg equations is derived firstly. Then, it is shown that the planar rarefaction wave is asymptotically stable in the case that the initial data are suitably small perturbations of the planar rarefaction wave. The proof is based on the delicate energy method. This is the first stability result of the planar rarefaction wave to the multi-dimensional viscous fluids with internal capillarity.

In [10], the modulation instability of two obliquely interacting waves in the presence of a thin pycnocline is investigated. Nonlinear evolution equations, correct up to the fourth order in wave steepness, are derived for a pair of obliquely interacting wave packets in the presence of thin pycnocline. These

evolution equations are then employed to perform stability analysis of a pair of obliquely interacting uniform wave trains. Figures plotted here reveal that the growth rate of instability decreases with the increase in pycnocline depth and also with the increase in density difference across the pycnocline. When the angle of interaction between the two wave packets is less than certain critical value the growth rate of instability decreases with the increase in angle and beyond this critical value the result is reversed.

The article [11] is devoted to the problem of propagation of weakly nonlinear wave-packets along contact surfaces in a three-layer hydrodynamic system “half space – layer – layer with rigid lid”. The condition of solvability of the problem in the third-order approximation is obtained, the evolution equation is derived in the form of a nonlinear Schrodinger equation and the modulation stability condition for its solutions is obtained. The stability diagram and its analysis are presented for the solution which takes place in the case of the balance between dispersion and non-linearity.

In article [12] the stability of wave packets propagation on the contact surface and free surface of hydrodynamic system “layer with rigid bottom – layer with free surface” was studied. The diagrams for nonlinear modulational stability for different thicknesses of lower layer were constructed. The presence of large regions of nonlinear modulational stability for capillary and gravitational waves for the different ratios of density and different thicknesses of two fluid layers was obtained. It was noted that the region of modulational nonlinear instability of the wave packet increased with decreasing of thickness of the lower layer.

In [13], the stability of wave packets propagating along the interface of two liquid layers with different densities taking into account surface tension forces is studied. The analysis is performed by the method of multiscale developments to the third order approximation. Characteristic diagrams of nonlinear stability as a function of the thickness of the lower layer are given. A significant redistribution of the regions of nonlinear stability with a change in the ratios of the thicknesses of the liquid layers was revealed.

In the study [15] the method of multiple scales is used to derive two partial differential equations that describe the evolution of two-dimensional wave-packets on the interface of two semi-infinite, incompressible, inviscid fluids of arbitrary densities, taking into account the effect of the surface tension. These differential equations can be combined to yield two alternate nonlinear Schrödinger equations; one of them contains only the first derivatives in time while the second contains the first and second derivatives in time. The first equation is used to show that the stability of uniform wavetrains depends on the wave length, the surface tension, and the density ratio. The results show that gravity waves are unstable for all density ratios except unity, while capillary waves are stable unless the density ratio is below approximately 0.1716. Moreover, the presence of surface tension results in the stabilization of some waves which are otherwise unstable. Although the first equation is valid for a wide range of wave numbers, it is invalid near the cutoff wave number separating stable from unstable motions. It is shown that the second Schrödinger equation is valid near the cutoff wave number and thus it can be used to determine the dependence of the cutoff wave number on the amplitude, thereby avoiding the usual process of determining a new expansion that is only valid near the cutoff conditions.

As can be seen from the above review, the study of wave motions and their characteristics in three-layer hydrodynamic systems is an urgent task of modern hydromechanics. The use of different approaches to modeling wave motions in three-layer systems makes it possible to analyze various aspects of the propagation of internal and surface waves. However, many unsolved questions remain, in particular the question of the modulation stability of wave packets in three-layer liquids.

This article is devoted to the study of modulation stability for the model of propagation of wave packets in a three-layer hydrodynamic system “layer with a solid bottom – layer – layer with a cover”.

2. Problem statement and research method

The problem of propagation of wave-packets of finite amplitude in a three-layer hydrodynamic system “layer with a hard bottom – liquid layer – layer with a cover” taking into account the force of surface

tensions on the contact surfaces is presented. Fluids are considered incompressible. The mathematical formulation of the problem is:

$$\begin{aligned} \varphi_{j,xx} + \varphi_{j,zz} &= 0 \quad \text{in } \Omega_j, \quad j = 1, 2, 3; \\ \eta_{1,t} - \varphi_{j,z} &= -\varphi_{j,x}\eta_{1,x} \quad \text{at } z = \eta_1(x, t), \quad j = 1, 2; \\ \eta_{2,t} - \varphi_{j,z} &= -\varphi_{j,x}\eta_{2,x} \quad \text{at } z = h_2 + \eta_2(x, t), \quad j = 2, 3; \\ \rho_1\varphi_{1,t} - \rho_2\varphi_{2,t} + g(\rho_1 - \rho_2)\eta_1 + \frac{1}{2}\rho_1(\nabla\varphi_1)^2 - \frac{1}{2}\rho_2(\nabla\varphi_2)^2 \\ &\quad - T_1(1 + (\eta_{1,x})^2)^{-3/2}\eta_{1,xx} = 0 \quad \text{at } z = \eta_1(x, t); \\ \rho_2\varphi_{2,t} - \rho_3\varphi_{3,t} + g(\rho_2 - \rho_3)\eta_2 + \frac{1}{2}\rho_2(\nabla\varphi_2)^2 - \frac{1}{2}\rho_3(\nabla\varphi_3)^2 \\ &\quad - T_2(1 + (\eta_{2,x})^2)^{-3/2}\eta_{2,xx} = 0 \quad \text{at } z = h_2 + \eta_2(x, t); \\ \varphi_{1,z} &= 0 \quad \text{at } z = -h_1; \\ \varphi_{3,z} &= 0 \quad \text{at } z = h_2 + h_3; \end{aligned}$$

φ_j ($j = 1, 2, 3$) are velocity potentials; η_1, η_2 are deviation of contact surfaces; T_1, T_2 are surface tension coefficients; g is acceleration of free fall; ρ_1, ρ_2, ρ_3 are densities of lower, middle and upper layers, respectively.

Using the method of multiscale developments for this problem, the first three approximations are obtained. The solutions of the first two approximations are also found and the solvability conditions for all three approximations are checked, the results are presented in article [14]. The evolution equation of the envelope on the lower surface of the contact has the form:

$$iA_{,t} + \omega' A_{,x} - 0.5\omega'' A_{,xx} = -\alpha^2 LA^2\bar{A},$$

where A is the envelope of the wave packets on the lower surface of the contact; \bar{A} is complex conjugate to A . Taking into account that

$$B = K_5 A,$$

where

$$K_5 = -\frac{\sinh(kh_2)((1 - \rho_2)k + T_1k^3 - \omega^2 \coth(kh_1) - \rho_2\omega^2 \coth(kh_2))}{\omega^2\rho_2}$$

the evolution equation for the upper contact surface is obtained:

$$iB_{,t} + \omega' B_{,x} - 0.5\omega'' B_{,xx} = -\alpha^2 \frac{L}{K_5^2} B^2\bar{B}$$

According to recent works [11–13, 15], the modulation stability conditions on the lower and upper surfaces, respectively, are as follows:

$$L\omega'' < 0, \tag{1}$$

$$\frac{L}{K_5^2}\omega'' < 0. \tag{2}$$

Since the coefficient K_5^2 is a non-negative expression that depends on the parameters ($h_1, h_2, h_3, \rho_2, \rho_3, T_1, T_2$), it does not affect the change of the sign in inequality (1)–(2). Therefore, to study modulation stability, we can limit ourselves to the study of condition (1).

3. Analysis of the modulation stability dependence on various physical parameters for the first pair of roots

Consider the graphs of the dependence of modulation stability limits and instability on the thickness of the lower layer $h_1 = 1, 4, 7, 10$ in the coordinate system (ρ_3, k) for the first pair of roots ω_1 (Figure 1). Other system parameters acquire the following values: $\rho_2 = 0.9, h_2 = 1, h_3 = 1, A = 1, \bar{A} = 1, T_1 = 0,$

$T_2 = 0$. In all cases, the modulation stability regions are designated “ MS_i ”, the modulation instability regions are designated “ MI_j ”.

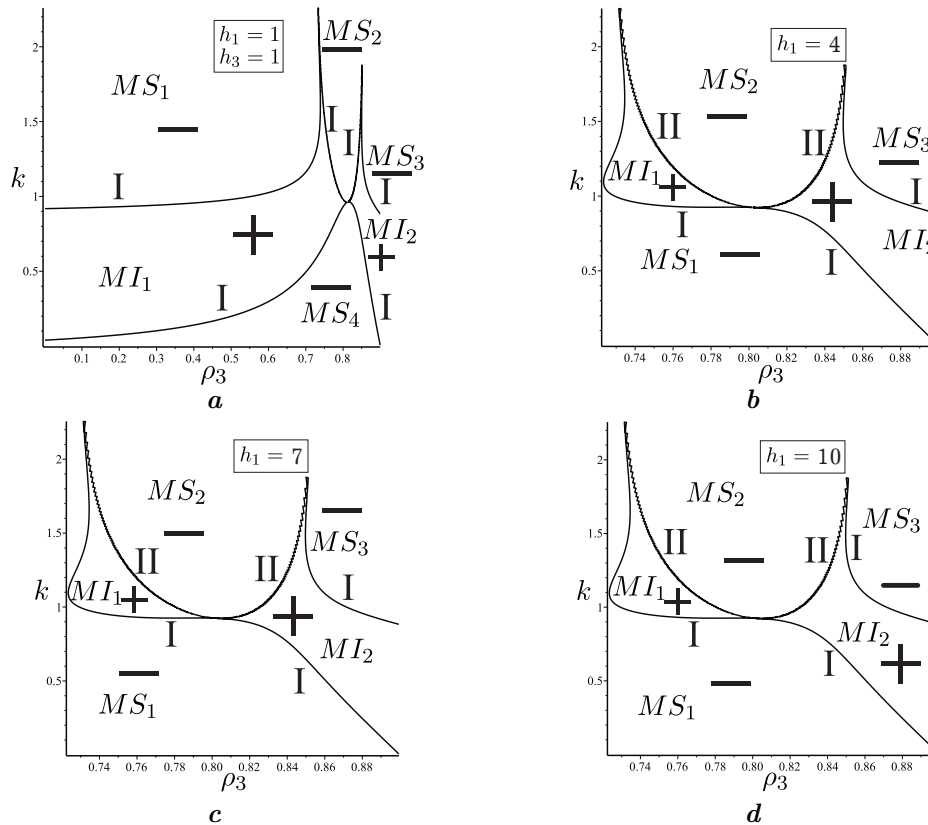


Fig. 1. Dependence of modulation stability on the thickness of the lower layer h_1 .

The graphs of the curves separating the regions of modulation stability and instability are described by equations $L\omega'' = 0$ and $L\omega'' \rightarrow \infty$. In the figures, these curves are marked “I” and “II”, respectively.

The graphs show that for $h_1 = 1$ (Figure 1a) there are two regions of modulation instability (MI_1 and MI_2) and four regions of modulation stability (MS_1, MS_2, MS_3, MS_4). At $h_1 = 1$ for long gravitational waves there is a region of modulation stability MS_4 . Also, the gravitational waves correspond to the region MI_1, MI_2 and MI_3 at $k < 1$. Capillary waves correspond to the region of stability MS_1, MS_2 and MS_3 at $k > 1$. At $h_1 = 4$ (Figure 1b), the modulation stability regions MS_1 and MS_4 are connected (the formed region is denoted by MS_1), then at $h_1 = 7$ (Figure 1c) and $h_1 = 10$ (Figure 1d) the boundaries of the modulation stability regions do not change. Therefore, there are three areas of modulation stability. For the stability regions MS_2 and MS_3 the situation for gravitational and capillary waves is similar to case 1a.

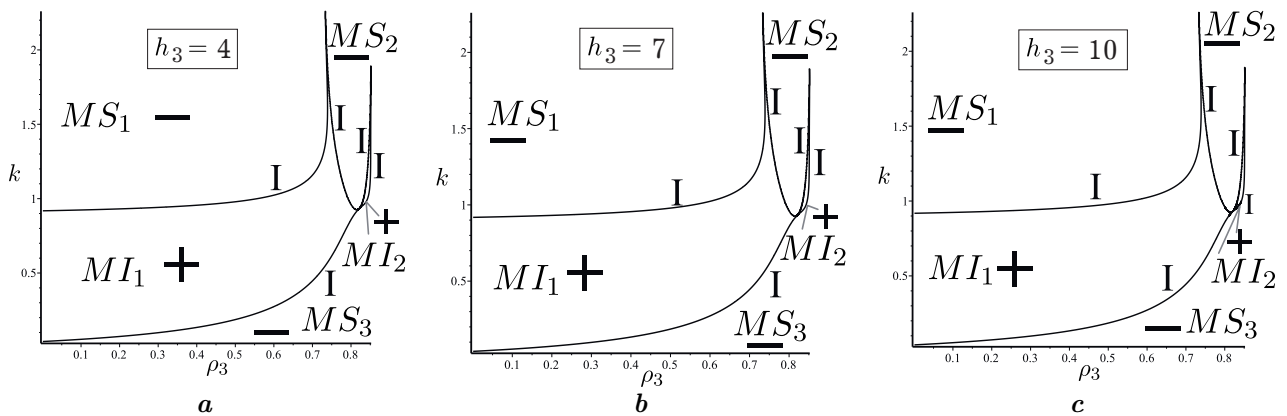


Fig. 2. Dependence of modulation stability on the thickness of the upper layer h_3 .

Figure 2 shows graphs of modulation stability and instability for the following values of the thickness of the upper layer $h_3 = 4, 7, 10$, respectively. Other system parameters acquire the following values: $\rho_2 = 0.9, h_1 = 1, h_2 = 1, A = 1, \bar{A} = 1, T_1 = 0, T_2 = 0$. The graphs show that for $h_3 = 4, 7, 10$ there are two regions of modulation instability (MI_1 and MI_2) and three regions of modulation stability (MS_1, MS_2, MS_3).

The limits of modulation stability and instability at all three values of the thickness of the upper layer h_3 do not change. Moreover, comparing these graphs with the case in Figure 1a, it is seen that two regions of modulation stability MS_3 and MS_4 merge into one (denoted by MS_3). The lower part of the modulation stability regions MS_1, MS_2 and MS_3 where $k < 1$ corresponds to the gravitational waves. For all three values of h_3 the capillary waves correspond to the regions of stability MS_1, MS_2 and MS_3 at $k > 1$. In the region of stability MS_3 with increasing ρ_3 gravitational waves turn into capillaries.

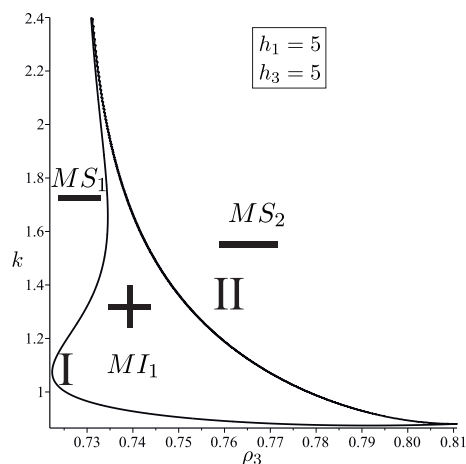


Fig. 3. Dependence of modulation stability on thicknesses h_1 and h_3 .

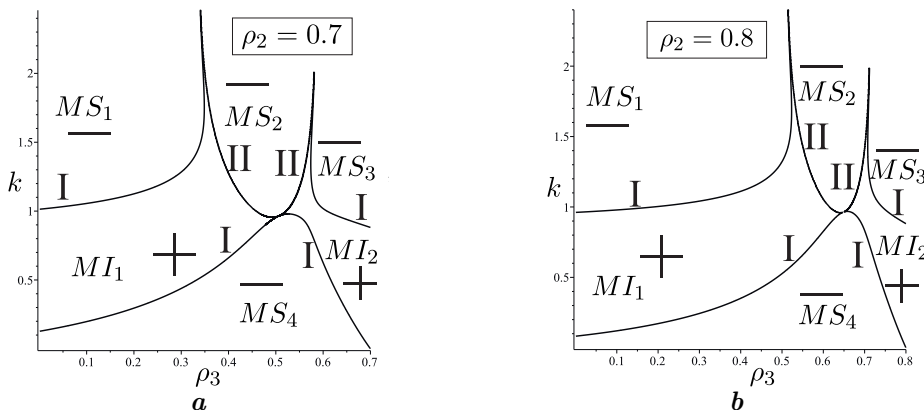


Fig. 4. Dependence of modulation stability on density thickness ρ_2 .

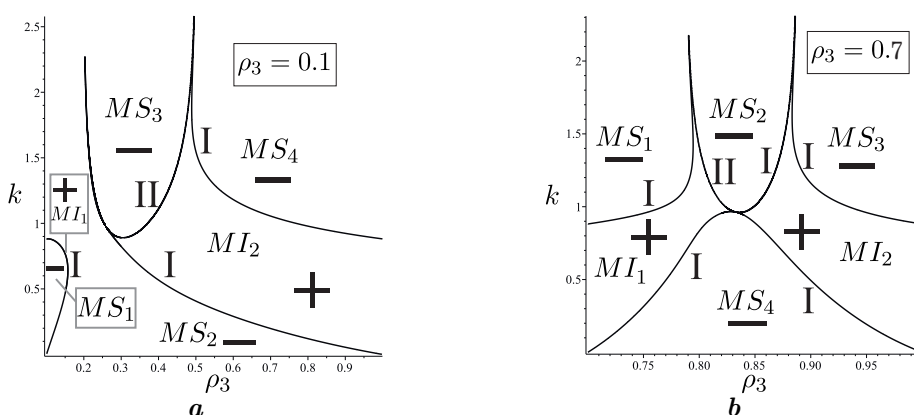


Fig. 5. Dependence of modulation stability on ρ_3 .

If we change the parameters $h_1 = 5$ and $h_3 = 5$ at the same time (Figure 3), then there is only one area of modulation instability MI_1 and two areas of modulation stability MS_1 and MS_2 . Gravitational waves correspond to both regions of modulation stability at $k < 1$. Capillary waves correspond to the regions of stability MS_1 and MS_2 where the value of the wave number $k > 1$.

Figure 4 shows the graphs of modulation stability at different values of the density of the middle layer ρ_2 . For this case, there are two areas of modulation instability MI_1, MI_2 and four areas of modulation stability MS_1, MS_2, MS_3 and MS_4 . In both graphs, the gravitational waves correspond to the region of modulation stability MS_4 and part of the regions MS_2 and MS_3 at $k < 1$. The capillary waves correspond to the stability region MS_1 and the regions MS_2 and MS_3 where $k > 1$.

Figure 5 shows diagrams of modulation stability and instability in the system (ρ_2, k) at the following values of the density of the upper layer $\rho_3 = 0.1, \rho_3 = 0.7$. The graph shows that in the case of $\rho_3 = 0.1$ (Figure 5a) there are four regions of modulation stability and two regions of modulation instability. The gravitational waves correspond to the modulation stability regions MS_2, MS_3 and MS_4 for $k < 1$ and the region MS_1 . In the area MS_2 gravitational waves turn into capillaries. The regions of modulation stability MS_2, MS_3 and MS_4 correspond to capillary waves for $k > 1$. Areas of modulation instability do not intersect. In the case of $\rho_3 = 0.7$ (Figure 5b) there are two regions of modulation instability and four regions of modulation stability. The regions of modulation stability MS_1, MS_2 and MS_3 for $k > 1$ correspond to capillary waves. The gravitational waves correspond to the regions of stability MS_1, MS_2, MS_3 at $k < 1$ and the region of modulation stability MS_4 .

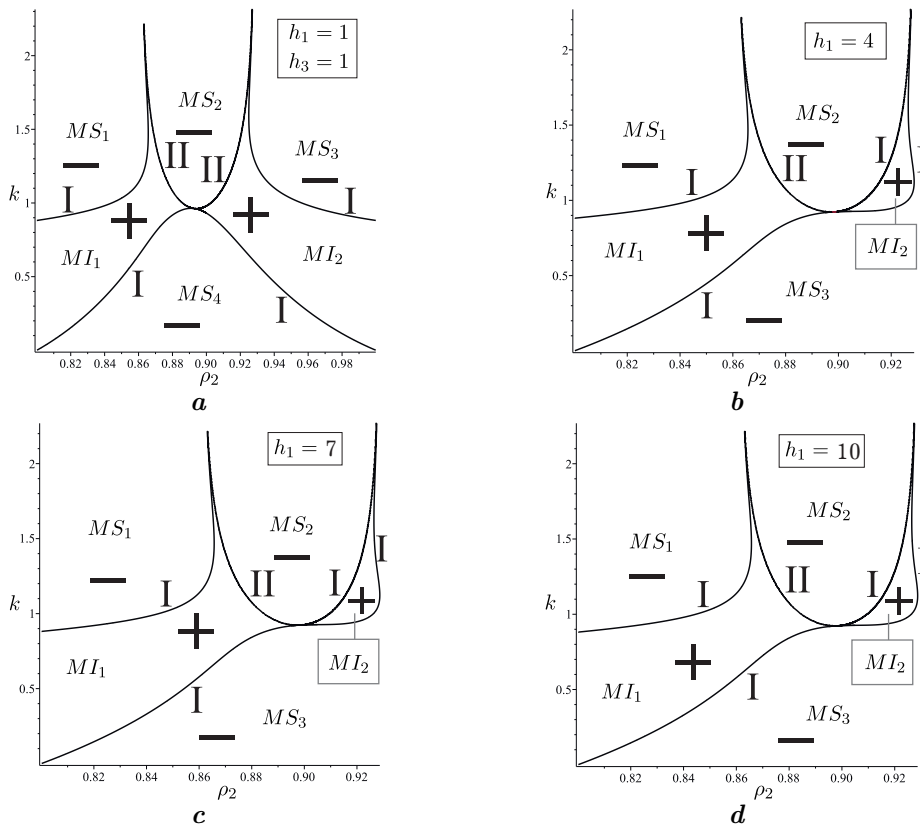


Fig. 6. Dependence of modulation stability on thickness h_1 in the system (ρ_2, k) .

Figure 6 shows the dynamics of changes in the boundaries of modulation stability and instability at different values of $h_1 = 1, 4, 7, 10$ in the system (ρ_2, k) , $\rho_3 = 0.8, h_3 = 1, h_2 = 1, A = 1, \bar{A} = 1, T_1 = 0, T_2 = 0$ are fixed system parameters.

At $h_1 = 1$ there are four regions of modulation stability and two regions of modulation instability. In this case, the region of stability MS_4 corresponds to gravitational waves. The regions of modulation stability MS_1, MS_2 and MS_3 correspond to capillary waves at $k > 1$, which turn into gravitational ones when $k < 1$. At $h_1 = 4, 7, 10$ (Figures 6b–6d) it is noticeable that two regions of modulation stability MS_3 and MS_4 merge into one (in Figures 6b–6d the formed region of stability is denoted by MS_3). Thus, the number of areas of modulation stability is reduced to three: MS_1, MS_2 and MS_3 . Also at $h_1 = 4, 7, 10$ the graphs of the limits of modulation stability and instability are the same.

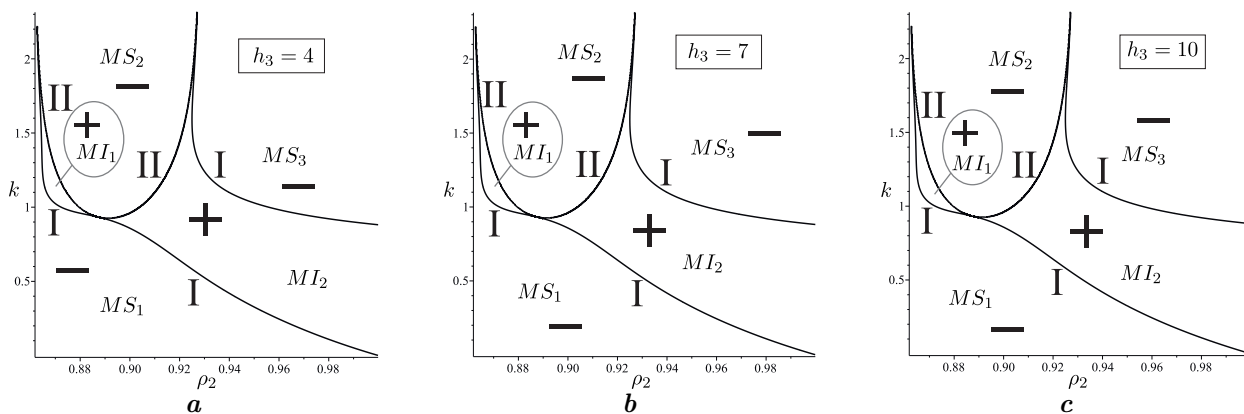


Fig. 7. Dependence of modulation stability on h_3 in the system (ρ_2, k) .

Figure 7 shows the dependence of the limits of modulation stability on the change in the thickness of the upper layer h_3 . The graphs show that for all three values of the thickness of the upper layer $h_3 = 4, 7, 10$ there are three areas of modulation stability and two areas of modulation instability. There is no change within the regions MS_1, MS_2 and MS_3 . Capillary waves correspond to all regions of stability at $k > 1$, gravitational waves correspond to all regions of stability at $k < 1$. If we compare these graphs with the case 6a ($h_3 = 1$), we see that two regions of modulation stability MS_1 and MS_4 merge into one, it is denoted by MS_1 .

4. Analysis of the modulation stability dependence on various physical parameter for the second pair of roots

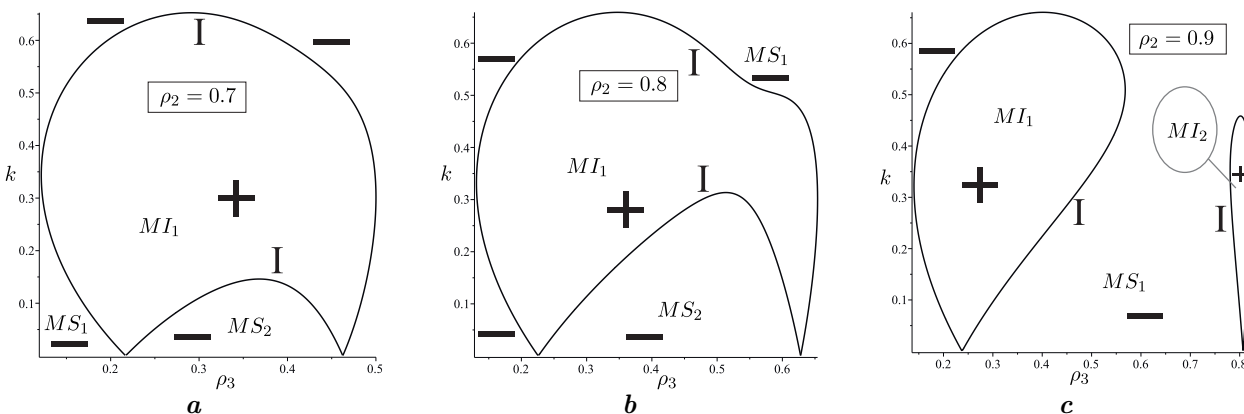


Fig. 8. Dependence of modulation stability on ρ_3 .

Consider the graphs of the dependence of modulation stability limits and instability on the density of the middle layer ρ_2 in the coordinate system (ρ_3, k) for the second pair of roots ω_2 (Figure 8). The following values are assigned to the fixed system parameters: $h_1 = 1, h_2 = 1, h_3 = 1, A = 1, \bar{A} = 1, T_1 = 0, T_2 = 0$. The regions of modulation stability and curves $L\omega'' = 0$ and $L\omega'' \rightarrow \infty$ are marked similarly to the previous paragraph.

In the case when $\rho_2 = 0.7$ (Figure 8a) there is one region of modulation instability MI_1 , which is closed, and two regions of modulation stability MS_1 and MS_2 . Moreover, the region of stability MS_1 surrounds the region of modulation instability MI_1 . Both regions of modulation stability correspond to gravitational waves. Similarly, to the previous case, for $\rho_2 = 0.8$ (Figure 8b) there are two regions of stability and one closed region of instability, the region of stability, MS_1 is around the region of modulation instability MI_1 . For $\rho_2 = 0.9$ (Figure 8c), the region of modulation instability is divided into two closed regions of instability MI_1 and MI_2 . In turn, the modulation stability regions MS_1 and MS_2 are interconnected (the resulting region is denoted by MS_1).

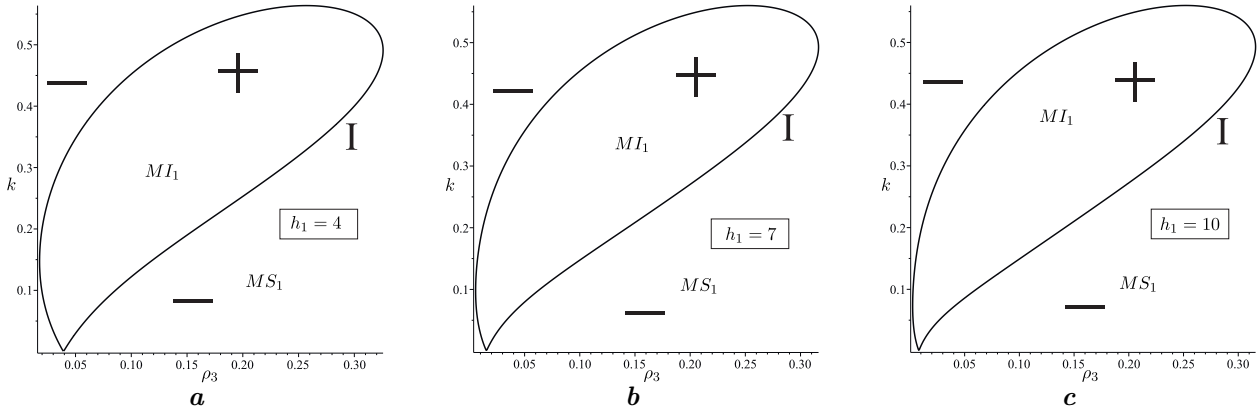


Fig. 9. Dependence of modulation stability on h_1 .

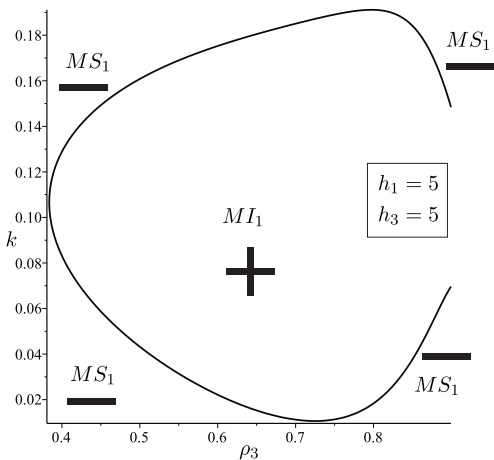


Fig. 10. Dependence of modulation stability on h_1 and h_3 .

Figure 9 illustrates the dynamics of changes in the boundaries of modulation stability and instability at different values of the thickness of the lower layer h_1 . Compared with the previous graph (Figure 8c), at $h_1 = 4, 7, 10$ the number of regions of modulation instability decreases to one closed region MI_1 . There is also one region of modulation stability MS_1 , that corresponds to gravitational waves.

Figure 10 shows a graph of the dependence of the modulation stability while increasing the thickness of the lower and upper layers by the values $h_1 = 5$ and $h_3 = 5$. Comparing the obtained graph with the previous graph in Figure 8c, it is seen that the two regions of modulation instability MI_1 and MI_2 merge into one, which is denoted by MI_1 . As in previous cases, the region of modulation stability MS_1 corresponds to gravitational waves.

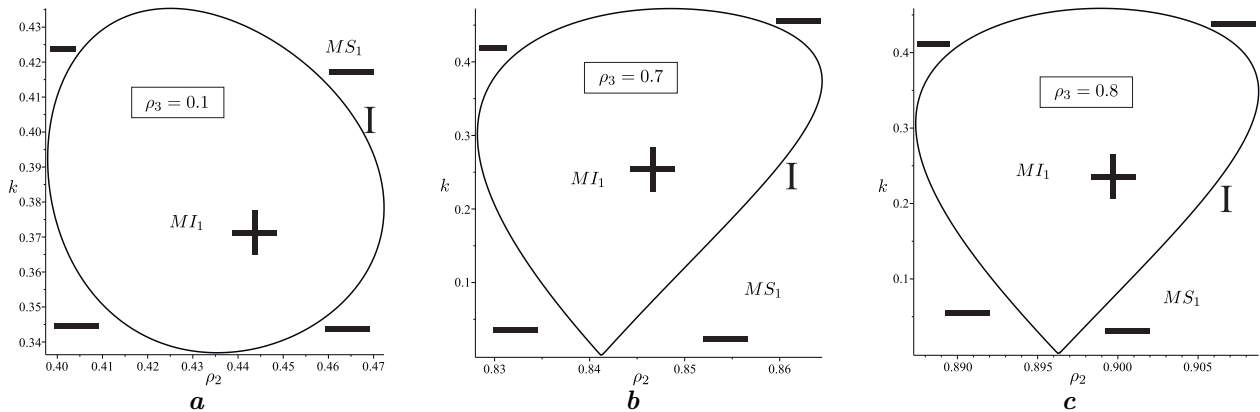


Fig. 11. Dependence of modulation stability on h_1 .

The graphs (Figure 11) of modulation stability and instability at different values of the density of the upper layer ρ_3 in the coordinate system (ρ_2, k) for the second pair of roots are given above, $h_1 = 1, h_2 = 1, h_3 = 1, A = 1, \bar{A} = 1, T_1 = 0, T_2 = 0$ are fixed values. In this case, for all three values of the density of the upper layer, there is one region of modulation stability and one region of modulation instability. The region MS_1 corresponds to gravitational waves. The modulation instability region is a closed region surrounded by a modulation stability region.

5. Conclusions

The evolutionary equations of the circumferential wave packets on the contact surfaces of the layers in the three-layer hydrodynamic system “layer with a solid bottom – layer – layer with a cover” were obtained. On the basis of evolutionary equations, a study of the modulation stability of wave packets was carried out. For this, stability diagrams were constructed. The presence of areas of modulation instability was revealed. It was established that the change in the density of the middle and upper layers significantly affects the size of these areas.

Analytical calculations and construction of modulation stability diagrams were performed using the Maple symbolic calculation package. The presented results were obtained for the first time among problems of this class and can be used in research related to the study of wave processes in the ocean, namely in areas of the ocean with three-layer density stratification.

-
- [1] Barros R., Choi W., Milewski P. A. Strongly nonlinear effects on internal solitary waves in three-layer flows. *Journal of Fluid Mechanics*. **883**, A16 (2020).
 - [2] Vincze M., Bozóki T. Experiments on barotropic-baroclinic conversion and the applicability of linear n -layer internal wave theories. *Experiments in Fluids*. **58**, 136 (2017).
 - [3] Talipova T., Kurkina O., Kurkin A., Didenkulova E., Pelinovsky E. Internal Wave Breathers in the Slightly Stratified Fluid. *Microgravity Science and Technology*. **32**, 69–77 (2020).
 - [4] Akylas T. R. David J. Benney: Nonlinear Wave and Instability Processes in Fluid Flows. *Annual Review of Fluid Mechanics*. **52**, 21–36 (2020).
 - [5] Wang L., Wang Z.-Z., Jiang D.-Y., Qi F.-H., Guo R. Semirational solutions and baseband modulational instability of the AB system in fluid mechanics. *European Physical Journal Plus*. **130**, 199 (2015).
 - [6] Hur V. M., Johnson M. A. Stability of periodic traveling waves for nonlinear dispersive equations. *SIAM Journal on Mathematical Analysis*. **47** (5), 3528–3554 (2015).
 - [7] Kharif C., Abid M., Carter J. D., Kalisch H. Stability of periodic progressive gravity wave solutions of the Whitham equation in the presence of vorticity. *Physics Letters A*. **384** (2), 126060 (2020).
 - [8] Chan H. N., Grimshaw R. H. J., Chow K. W. Modeling internal rogue waves in a long wave-short wave resonance framework. *Physical Review Fluids*. **3** (12), 124801 (2018).
 - [9] Li Y. P., Chen Z. Z., Luo Z. Stability of the planar rarefaction wave to two-dimensional Navier–Stokes–Korteweg equations of compressible fluids. *Mathematical Methods in the Applied Sciences*. **43** (6), 3307–3330 (2020).
 - [10] Purkait A., Debsarma S. Modulational instability of two obliquely interacting waves in presence of a thin pycnocline. *European Journal of Mechanics – B/Fluids*. **84**, 517–527 (2020).
 - [11] Avramenko O., Lunyova M. Modulation stability of wave packets in a three-layer hydrodynamic system. *Bulletin Taras Shevchenko National University of Kyiv Mathematics Mechanics*. **1**, 30–35 (2019), (in Ukrainian).
 - [12] Avramenko O., Naradovyy V. Stability of wave-packets in the two-layer fluid with free surface and rigid bottom. *Contemporary Problems of Mathematics, Mechanics and Computing Sciences*. **1**, 5–12 (2011).
 - [13] Selezov I. T., Avramenko O. V., Gurtovyi Yu. V. Nonlinear stability of wave packet propagation in a two-layer liquid. *Prikl. Gidromekh.* **8** (80), 60–65 (2006).
 - [14] Naradovyi V. V., Kharchenko D. Investigation of the energy of wave motions in a three-layer hydrodynamic system. *Waves in Random and Complex Media*. **31** (6), 1729–1748 (2019).
 - [15] Nayfeh A. H. Nonlinear Propagation of Wave-Packets on Fluid Interfaces. *Journal of Applied Mechanics*. **43** (4), 584–585 (1976).

Модуляційна стійкість хвильових пакетів у тришаровій рідині

Харченко Д. С., Наратовий В. В.

*Центральноукраїнський державний університет імені Володимира Винниченка,
вул. Шевченка, 1, 25000, Кіровоградський, Україна*

В даній статті досліджується умова модуляційної стійкості для задачі поширення хвильових пакетів у тришаровій гідродинамічній системі “шар з твердим дном – шар – шар з кришкою”. Проілюстровано та проаналізовано графіки залежності меж модуляційної стійкості від товщини нижнього і верхнього шару та від густини середнього і верхнього шарів для капілярних та гравітаційних хвиль. Отримані еволюційні рівняння обвідних хвильових пакетів у вигляді нелінійного рівняння Шредінгера другого порядку для нижньої та верхньої поверхонь контакту. Виведено умови модуляційної стійкості.

Ключові слова: *хвильові пакети; модуляційна стійкість; гравітаційні хвилі.*